Bioorganic & Medicinal Chemistry 21 (2013) 3154–3163

Contents lists available at SciVerse ScienceDirect

Bioorganic & Medicinal Chemistry

journal homepage: www.elsevier.com/locate/bmc

Selective CB2 agonists with anti-pruritic activity: Discovery of potent and orally available bicyclic 2-pyridones

Ken-ichi Kusakabe [a,*], Yasuyoshi Iso [a], Yukio Tada [a], Masahiro Sakagami [a], Yasuhide Morioka [a], Nobuo Chomei [a], Satomi Shinonome [a], Keiko Kawamoto [a], Hideyuki Takenaka [a], Kiyoshi Yasui [a], Hiroshi Hamana [b], Kohji Hanasaki [a]

[a] Medicinal Research Laboratories, Shionogi Pharmaceutical Research Center, 11-1 Futaba-cho 3-chome, Toyonaka, Osaka 561-0825, Japan
[b] Faculty of Pharmacy, Chiba Institute of Science, 15-8 Shiomi-cho, Choshi, Chiba 288-0025, Japan

ARTICLE INFO

Article history:
Received 4 January 2013
Revised 15 March 2013
Accepted 16 March 2013
Available online 30 March 2013

Keywords:
Cannabinoid
CB2
Agonist
Pruritus
Itch
Pyridone
Pyridine-2-one
Homology model

ABSTRACT

The CB2 receptor has emerged as a potential target for the treatment of pruritus as well as pain without CB1-mediated side effects. We previously identified 2-pyridone derivatives **1** and **2** as potent CB2 agonists; however, this series of compounds was found to have unacceptable pharmacokinetic profiles with no significant effect in vivo. To improve these profiles, we performed further structural optimization of **1** and **2**, which led to the discovery of bicyclic 2-pyridone **18e** with improved CB2 affinity and selectivity over CB1. In a mouse pruritus model, **18e** inhibited compound 48/80 induced scratching behavior at a dose of 100 mg/kg. In addition, the docking model of **18e** with an active-state CB2 homology model indicated the structural basis of its high affinity and selectivity over CB1.

1. Introduction

Atopic dermatitis (AD) is a chronic and relapsing inflammatory skin disease that is characterized by intense itching (pruritus), dry skin, redness and exudation.[1,2] The often unbearable pruritus experienced by AD patients led it to be referred to commonly as 'the itch that rashes'. Another common feature of AD is the itch–scratch–itch cycle. Scratching further intensifies the itch and damages the skin, which in turn increases inflammation and the establishment of an itch–scratch–itch cycle plays a key role in increasing the severity of AD.[3] Although itching is one of the principal symptoms of AD, there is a lack of therapeutic drugs that can quickly and effectively tackle the itch associated with it.[4]

Both cannabinoid receptors CB1 and CB2 are expressed on cutaneous sensory nerve fibers, mast cells, and keratinocytes.[2] The involvement of cannabinoid receptors in reducing pruritus has been shown in itch models.[5,6] For example, peripheral administration of cannabinoid agonist HU-210 has been shown to attenuate histamine-induced itch in humans.[5] Furthermore, the CB2 agonist has reduced pruritus in patients with AD, lichen simplex, and CKD-associated pruritus.[1] Unlike CB2 agonists, the CB1 agonist acts on the central CB1 receptor to cause central nervous system (CNS) mediated effects such as catalepsy, hypothermia and hypoactivity. Thus, selective CB2 agonists should be useful against pruritus without CB1-mediated side effects.

A number of CB2 selective agonists have been reported on from various studies.[9] For example, HU-308,[7] AM1241,[8] and GW842166X[9b] are well-known selective CB2 agonists that are active in animal models of pain. We recently reported the discovery of pyridone-based CB2 agonists **1** and **2** designed from an isoquinolone based screening hit (Fig. 1),[10] but this series of compounds was found to have unacceptable pharmacokinetic profiles (**2**: $F = 8.2\%$; CL = 119 mL/min/kg in rat), which resulted in no significant effect in vivo. Therefore, in our research, we decided to try to discover selective CB2 agonists with in vivo activity. Herein, we report the identification and optimization of bicyclic 2-pyridone derivatives. Our effort led to the discovery of **18e** as a potent,

Abbreviations: AD, atopic dermatitis; CB, cannabinoid; cAMP, adenosine 3′,5′-cyclic monophosphate; CNS, central nervous system; CHO, Chinese hamster ovary; DCM, dichloromethane; DMF, *N*,*N*-dimethylformamide; ECL, extracellular loop; EtOAc, ethyl acetate; SAR, structure–activity relationship; TEA, triethylamine; THF, tetrahydrofuran; TM, transmembrane helix.

* Corresponding author. Tel.: +81 6 6331 6190; fax: +81 6 6332 6385.
E-mail address: ken-ichi.kusakabe@shionogi.co.jp (K. Kusakabe).

0968-0896/$ - see front matter © 2013 Published by Elsevier Ltd.
http://dx.doi.org/10.1016/j.bmc.2013.03.030

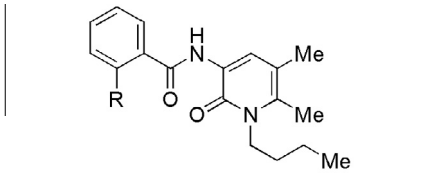

Figure 1. Lead compounds **1** and **2**.

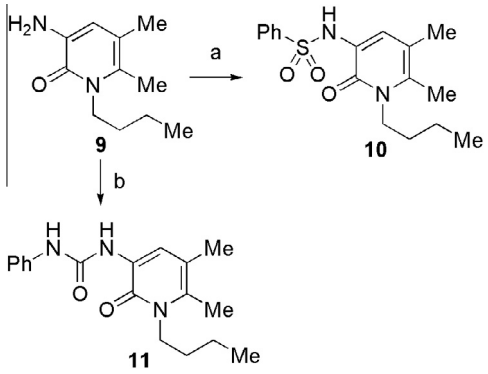

Scheme 1. Reagents and conditions: (a) benzenesulfonyl chloride, pyridine, THF, 0 °C (70%); (b) phenyl isocyanate, THF, rt (94%).

selective, and orally available CB2 agonist, which was active in a mouse pruritus model. We also predicted a binding mode of **18e** in a CB2 homology model, which explained its high affinity for CB2 and selectivity over CB1.

2. Chemistry

The syntheses of **10** and **11** are illustrated in Scheme 1. Amine **9** was treated with benzenesulfonyl chloride in THF to give compound **10**. Urea **11** was prepared by the reaction of **9** with phenyl isocyanate. As shown in Scheme 2, condensation of acid **12** with benzyl amine gave compound **13**.

The syntheses of **18a** and bicyclic pyridones **18b**–**e** proceeded as shown in Scheme 3. Ketones **14a**–**e** were condensed with *n*-butylamine to give the corresponding ketimines, which were

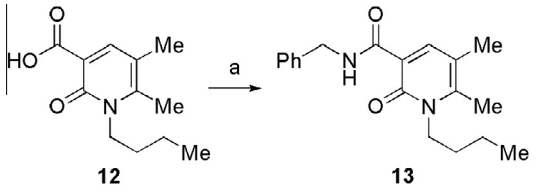

Scheme 2. Reagents and conditions: (a) DCC, HOBt, benzylamine, THF, rt (27%).

cyclized by treatment of malonate **15** to yield esters **16a**–**e**. Hydrolysis of the esters in **16a**–**e** followed by reactions of corresponding acid chlorides with benzyl amine resulted in the final compounds **18a**–**e**. Preparation of pyridones **21a**–**c** was conducted in a similar manner to that of **18a**–**e** (Scheme 4). Scheme 5 also depicts the synthesis of **22a**–**f**. Finally, carboxylic acid **17e** was coupled with various amines to give the final compounds **22a**–**f**.

3. Results and discussion

3.1. Optimization of lead 1 and identification of bicyclic 2-pyridone 18e

We first explored the effects of the linker groups at the C3 position (Table 1). Replacement of the amide group with 'reversed' benzyl amide led to analog **13** that had similar CB2 potency as benzamide **1**. However, changes, such as replacement of the benzamide with either sulfonamide or urea, resulted in a dramatic loss of activity, as suggested by compounds **10** and **11**. Benzamide **1** and 'reversed' benzyl amide **13** were nearly equipotent, and we selected 'reversed' benzylamide for further optimization due to its synthetic accessibility.

To improve CB2 affinity and selectivity over CB1, substitutions at the 5- and 6-positions of pyridone ring were investigated (Table 2). Replacement of the methyl group at the 6-position with a slightly larger ethyl group (**18a**) led to a threefold increase in activity. Introduction of a cyclopentyl ring at the 5- and 6-positions gave rise to bicyclic pyridone **18b**, which was equipotent with monocyclic **18a**, but both compounds (**18a** and **18b**) showed no improvement in selectivity over CB1 as compared to **13** (16-fold and 8.9-fold, respectively). It was gratifying to see that compound **18c** with a cyclohexyl ring showed improved selectivity (44-fold) over CB1, and retained good CB2 affinity with agonist activity (CB2 Ki = 17 nM; CB2 cAMP IC_{50} = 17 nM). Encouraged by this re-

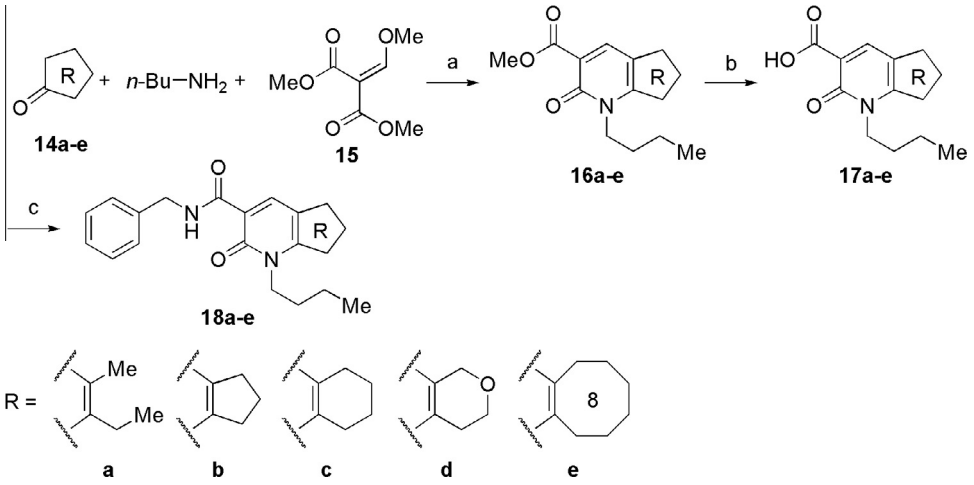

Scheme 3. Reagents and conditions: (a) (i) compounds **14a**–**g**, *n*-$BuNH_2$, toluene, reflux, (ii) compound **15**, diglyme, 120 °C (71%); (b) NaOH, EtOH, rt (88%); (c) (i) thionyl chloride, DMF, toluene, 75 °C, (ii) benzylamine, DCM, rt (70%).

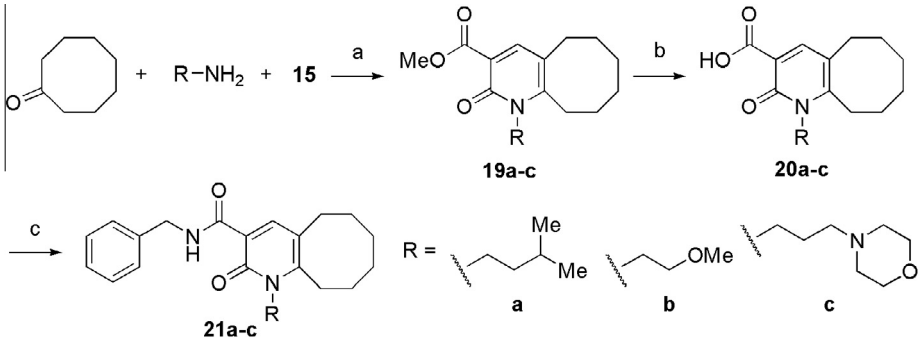

Scheme 4. Reagents and conditions: (a) (i) cyclooctanone, R-NH_2, toluene, reflux, (ii) **15**, diglyme, 120 °C (47%); (b) NaOH, EtOH, rt (86%); (c) (i) thionyl chloride, DMF, toluene, 75 °C, (ii) benzylamine, DCM, rt (97%).

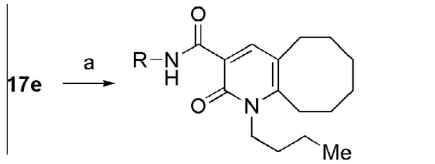

22a: R = H
22b: R = i-Pr
22c: R = Cyclohexyl
22d: R = N-Methylpiperidin-4-yl
22e: R = Cumyl
22f: R = 2-Phenethyl

Scheme 5. Reagents and conditions: (a) (i) thionyl chloride, DMF, toluene, 75 °C, (ii) R-NH_2, DCM, rt (87%).

sult, a number of bicyclic pyridones were also investigated. As a general trend, expanding ring size led to an increase in affinity. For example, bicyclic pyridones containing cycloheptane and cyclodecane resulted in an improvement in CB2 affinity (6.0 nM and 2.5 nM, respectively; data not shown). Finally, compound **18e**, bearing a cyclooctane ring on the pyridone ring, showed the best affinity and selectivity (CB2 Ki = 1.5 nM; 593-fold selectivity) compared with other bicyclic pyridones. In contrast, introduction of an oxygen atom at the bicyclic pyridone ring of **18c** caused a dramatic loss in activity as shown by **18d**, suggesting that introduction of hydrophobic group significantly contributes to an increase in CB2 affinity of this series of analogues.

Having identified the optimal bicyclic pyridone scaffold (**18e**), we next investigated substitutions at the pyridone N-1 position (Table 3). The isopentyl analog **21a** had high affinity for CB2, but failed to exhibit selectivity for CB2. The methoxyethyl analog **21b** was equipotent with the *n*-butyl analog **18e**. In contrast, there was a marked decrease in activity when a morpholinopropyl group was introduced (**21c**), indicating that increased polarity in this region reduced CB2 affinity. Taken together, the *n*-butyl group was found to be the optimal choice.

Using the optimal side chain and scaffold, we shifted our attention to exploring the amide side chain of the pyridone ring (Table 4). Exploration of this region revealed that hydrophobic substituents led to increased affinity for both CB2 and CB1. For example, removing the benzyl substituent of **18e**, as with compound **22a**, caused reduction in activity. Introduction of a hydrophobic substituent such as an isopropyl group (**22b**) led to a 10-fold increase in affinity for CB2 and CB1 compared to unsubstituted **22a**. Introduction of additional hydrophobicity with a cyclohexyl group (**22c**) gave an impressive further 20-fold increase in CB2 potency over **22b** while maintaining a 95-fold selectivity over CB1. Installation of a gem-dimethyl group at the benzylic

Table 1
SAR of the 3-position on the pyridione ring

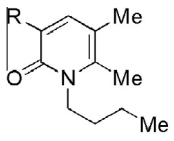

Compd	R	hCB2 Ki (nM)	hCB1 Ki[a] (nM)
1	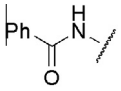	89	1376
10	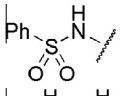	>5000	NT
11	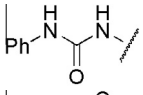	>5000	NT
13	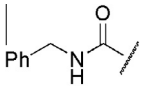	66	606

[a] NT = not tested.

position in **18e**, compound **22e**, resulted in a 15-fold increase in activity, but **22e** also exhibited high affinity for CB1 (Ki = 1.0 nM). These results suggested that a lipophilic substituent next to the nitrogen of the amide bond was important for both CB1 and CB2 affinity, but particularly for CB1. Replacement of the benzyl side chain with 2-phenethyl led to compound **22f** that had a similar level of CB2 potency and selectivity for CB1 as the benzyl analog **18e**. Finally, benzylamide **18e** and cyclohexylamide **22c** were notable for their high CB2 potency and moderate to high selectivity for CB1, and thus were selected for further in vivo evaluation.

3.2. Putative binding mode of 18e in an active-state CB2 homology model

To better understand the SAR results and these binding modes, we performed a modeling analysis of compound **18e** using a CB2 homology model. In our previous paper,[10] we constructed a CB2 homology model using the crystal structure of the β_2 adrenergic receptor–Gs protein complex[14] as a template and also reported the

Table 2
SAR of the A ring on the bicyclic pyridone ring

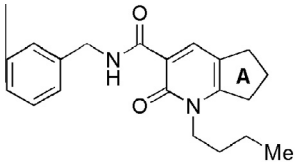

Compd	A	hCB2 Ki (nM)	hCB2 cAMP IC_{50}[a] (nM)	hCB1 Ki[a] (nM)	hCB1/hCB2[b]
18a	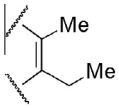	20	NT	322	16
18b[c]	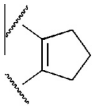	16	NT	143	8.9
18c[c]	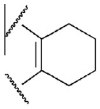	17	17	746	44
18d	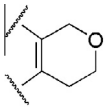	204	NT	NT	ND
18e[c]	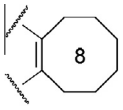	1.5	1.4	890	593

[a] NT = not tested.
[b] ND = not determined.
[c] E_{max} (%) is the maximum inhibition rate against forskolin-induced cAMP production at indicated concentration. E_{max} values for selected compounds were determined: **18b**: 83% at 2 μM, **18c**: 76% at 2 μM, **18e**: 100% at 0.2 μM.

Table 3
SAR of N-1 position on the bicyclic pyridone

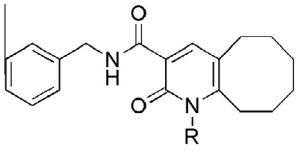

Compd	R	hCB2 Ki (nM)	hCB1 Ki[a] (nM)	hCB1/hCB2[b]
18e	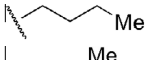	1.5	890	593
21a	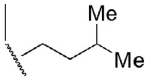	0.9	9.0	10
21b	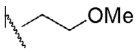	8.0	1769	221
21c	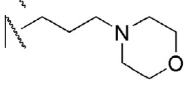	209	NT	ND

[a] NT = not tested.
[b] ND = not determined.

Table 4
SAR of C-3 amide derivatives

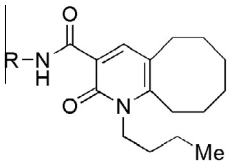

Compd	R	hCB2 Ki (nM)	hCB2 cAMP IC_{50}[a] (nM)	hCB1 Ki[a] (nM)	hCB1/hCB2[b]
18e[c]	Benzyl	1.5	1.4	890	593
22a	H	40	NT	>5000	>125
22b[c]	*i*-Pr	4.0	2.5	591	148
22c[c]	Cyclohexyl	0.2	<0.2	19	95
22d	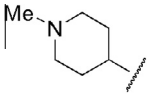	147	NT	NT	ND
22e	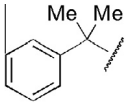	0.1	0.2	1.0	1.0
22f[c]	2-Phenethyl	1.6	1.7	908	568

[a] NT = not tested.
[b] ND = not determined.
[c] E_{max} (%) is the maximum inhibition rate against forskolin-induced cAMP production at indicated concentration. E_{max} values for selected compounds were determined: **18e**: 100% at 0.2 μM, **22b**: 92% at 2 μM, **22c**: 98% at 0.02 μM, **22f**: 98% at 0.2 μM.

docking model of **2** with the CB2 model. Using the CB2 homology model, pyridone **18e** was docked using ASEDock.[15] The binding mode of **18e** is essentially identical to that of **2** (Fig. 2a). The amide group of **18e** forms a hydrogen bond between the amide carbonyl and the hydroxyl group of $S193^{5.42}$ (superscripts indicate Ballesteros–Weinstein numbers[20]) (Fig. 2b and c). The phenyl ring displays van der Waals interactions with $T114^{3.33}$ and $Y190^{5.39}$. The cyclooctane ring lies in a hydrophobic pocket defined by $F197^{5.46}$, $W258^{6.48}$, $V261^{6.51}$, and $C288^{7.42}$. The pyridone ring shows π–electron stacking interactions with $W194^{5.43}$. The N-1 *n*-butyl chain fits well in a pocket formed by $V113^{3.32}$, $F117^{3.36}$, $F281^{7.35}$, and $S285^{7.39}$.

The 'reversed' amide **13** was equipotent with the 'normal' amide **2** as shown in Table 1. An overlap of 'reversed' amide **18e** (blue) and **2** (yellow) in CB2, as shown in Figure 2a, reveals that both amide carbonyl groups are directed toward the OH of $S193^{5.42}$ and form the hydrogen bonding interactions. This may contribute to the nearly equipotent activity. Unlike the amide carbonyl groups, the amide side chains are located in different regions. The benzyl group of **18e** is oriented toward $Y190^{5.39}$ in transmembrane helix (TM) 5, while the phenyl ring of **2** is located in the TM4-second extracellular loop (ECL2)-TM5 region. The SAR of **2** was very sensitive around the phenyl ring as reported in our previous paper,[10] while that of **18e** was well tolerated around the benzyl group as shown in Table 2. These differences in the SAR between the 'reversed' and 'normal' amides may result from the differences in location and vector of the amide side chains in the pocket.

Introduction of alkyl chains or rings on the pyridone (**18a**, **18b**, **18c**, and **18e**) led to an increase in CB2 affinity as compared with dimethyl derivative **13**. The docking model of **18e** with CB2 showed that the cyclooctane ring fits well in this hydrophobic pocket to create van der Waals contact with non-conserved $F197^{5.46}$, which is valine in CB1 (Fig. 2b). This observation explains why **18e** is more potent as well as selective for CB1. In contrast, incorporation of the hydrophilic tetrahydropyranyl ring on the pyridone (**18d**) resulted in a 136-fold decrease in CB2 affinity as compared with **18e**. As mentioned above, there are hydrophobic residues in this area, which explains the loss of potency in **18d**.

3.3. Pharmacokinetics and in vivo efficacy

We conducted a pharmacokinetic study of CB2 agonists **18e** and **22c** in mice (Table 5). When given orally (10 mg/kg), **22c** exhibited an oral bioavailability of 48% and an AUC of 6917 ng h/mL. This compound also showed a good clearance of 35 mL/min/kg with iv dosing. On the other hand, **18e** had lower oral bioavailability (25%) and higher clearance (96 mL/min/kg). To evaluate these compounds in a mouse model, we examined the mouse CB1 and CB2 affinity (Ki) of **18e** and **22c**. These compounds showed similar potency for mouse and human CB2, but **22c** showed a further increase in affinity for CB1 (Ki = 12 nM). Therefore, we selected **18e** for further in vivo pharmacological evaluation.

The anti-pruritic effect of **18e** was evaluated in a mouse pruritus model. This experiment was carried out by the method of Inagaki et al.[16] with some modifications. The backs of ICR strain mice were clipped, and compound 48/80 was injected intradermally to elicit the response. The scratching behavior of the mice was observed immediately after the injection, and the number of times that the mice scratched itself was counted for 30 min. Evaluation of the inhibitory effects against pruritus was performed by comparing the number of times the mice scratched in the compound-administered group with that in the vehicle-administered group. Orally administered **18e** at a dose of 100 mg/kg inhibited the scratching behavior induced by compound 48/80 (81% inhibition). Furthermore, **18e** did not show any decrease in locomotor activity which was considered to be a CB1-mediated CNS side effect.

4. Conclusions

A series of bicyclic 2-pyridone derivatives were identified as selective CB2 agonists. Incorporation of the cyclooctane ring on the pyridone core was crucial to achieving both high affinity for

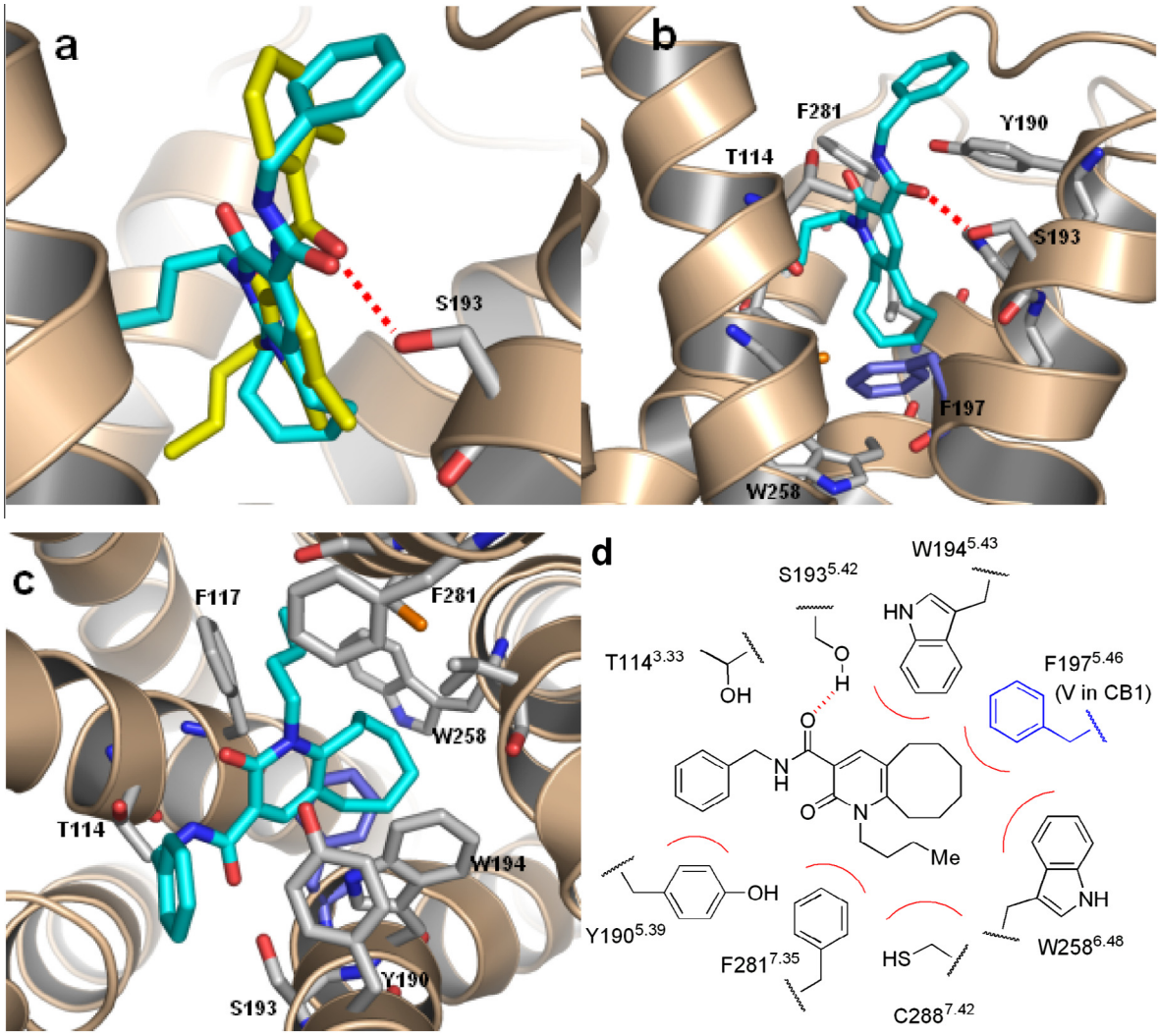

Figure 2. (a) Overlay of **2** (yellow) and **18e** (cyan) in CB2 homology model (side view with TM4 in front). Hydrogen bonds with S193$^{5.42}$ (white) are shown. (b) Docking model of **18e** (cyan) with CB2 (side view with TM4 in front). F197$^{5.46}$ (blue) and key residues (white) are shown. (c) Docking model of **18e** (cyan) with CB2 (extracellular view). (d) Diagram of **18e** in the binding pocket. Hydrophobic interactions are shown as red lines and the hydrogen bond appear as dotted red lines. Figures a–c were generated with PyMOL.[21]

Table 5
Pharmacokinetic properties of **18e** and **22d** in mice

Compd	iv (1 mg/kg[a] or 2 mg/kg[b])			po (30 mg/kg)		
	V_{dss}[c] (L/kg)	CL_{total}[d] (mL/min/kg)	$t_{1/2}$[e] (h)	AUC[f] (ng h/mL)	C_{max}[g] (ng/mL)	F[h] (%)
18e	2.29	96	0.28	390	168	25
22c	0.89	35	0.30	6917	1845	48

[a] Compound **22c**.
[b] Compound **18e**.
[c] Volume of distribution.
[d] Total plasma clearance.
[e] Half-life.
[f] Area under the curve.
[g] Maximum plasma concentration.
[h] Oral bioavailability.

CB2 and CB2 selectivity for CB1. This effort led to potent and selective CB2 agonists **18e** and **22c** with moderate to good bioavailability, and **18e** had high potency in the itch model induced by compound 48/80. In addition, the docking model of **18e** with our active-state CB2 homology model indicated the structural basis of its high affinity and selectivity over CB1. Further studies on SAR around these compounds led to the discovery of the clinical candidates S-777469[18] and S-444823.[19]

5. Experimental section

5.1. General chemistry

All commercial reagents and solvents were used as received unless otherwise noted. Thin layer chromatography (TLC) analysis was performed using Merck silica gel 60 F_{254} thin layer plates

(250 μm thickness). Flash column chromatography was carried out on an automated purification system using Yamazen prepacked silica gel columns. ^{1}H NMR spectra were recorded on a Varian Gemini 300 MHz. Spectral data are reported as follows: chemical shift (as ppm referenced to tetramethylsilane), multiplicity (s = singlet, d = doublet, dd = double doublets, dt = double triplet, t = triplet, q = quartet, m = multiplet, br = broad peak), coupling constant, and integration value. Analytical LC/MS was performed on a Waters X-Bridge (C18, 5 μm, 4.6 mm × 50 mm, a linear gradient from 10% to 100% B over 3 min and then 100% B for 1 min (A = H_2O + 0.1% formic acid, B = MeCN + 0.1% formic acid), flow rate 3.0 mL/min) using a Waters system equipped with a ZQ2000 mass spectrometer, 2525 binary gradient module, 2996 photodiode array detector (detection at 254 nm), and 2777 sample manager. IR spectra were recorded on a Nicolet 20SXB FT-IR spectrometer. HRMS-FAB spectra were measured on a JEOL JMS-SX/SX102A.

5.1.1. *N*-(1-Butyl-5,6-dimethyl-2-oxo-1,2-dihydropyridin-3-yl)benzenesulfonamide (10)

To a solution of **9** (78 mg, 0.40 mmol) in pyridine (1 mL) was added a solution of benzenesulfonyl chloride (60 μL, 0.47 mmol, 1.2 equiv) in THF (1 mL) at 0 °C. The mixture was stirred at 0 °C for 1 h, and diluted with H_2O and EtOAc. The aqueous layer was separated and extracted with EtOAc. The combined organic extracts were washed with 1 M HCl solution, H_2O and saturated aqueous $NaHCO_3$ solution, dried over $MgSO_4$, filtered and concentrated. The residue was diluted with ethyl ether, and resulting solid was collected on a glass filter. The solid was recrystallized from CH_2Cl_2/ethyl ether to give **10** (94 mg, 70%) as a tan solid. Mp 170–171 °C. ^{1}H NMR (300 MHz, $CDCl_3$) δ 0.92 (t, J = 7.2 Hz, 3H), 1.25–1.37 (m, 2H), 1.45–1.55 (m, 2H), 2.08 (s, 3H), 2.23 (s, 3H), 3.97 (t, J = 7.8 Hz, 2H), 7.35 (s, 1H), 7.41–7.55 (m, 2H), 7.65 (br s, 1H), 7.83–7.87 (m, 2H). Anal. calcd for $C_{17}H_{22}N_2O_3S$: C, 61.05; H, 6.63; N, 8.38; S, 9.59. Found: C, 60.98; H, 6.71; N, 8.35; S, 9.53.

5.1.2. 1-(1-Butyl-5,6-dimethyl-2-oxo-1,2-dihydropyridin-3-yl)-3-phenylurea (11)

To a solution of **9** (54 mg, 0.278 mmol) in THF (1.5 mL) was added a solution of phenyl isocyanate (37 mg, 0.311 mmol, 1.1 equiv) in THF (1.5 mL) at room temperature. The mixture was stirred overnight at room temperature and evaporated. The residue was diluted with methanol, and added activated carbon was added. The suspension was filtered, and the filtrate was evaporated. The resulting solid was crystallized from CH_2Cl_2/ethyl ether to give **11** (82 mg, 94%) as a tan solid. Mp 208–209 °C. ^{1}H NMR (300 MHz, $CDCl_3$) δ 1.00 (t, J = 7.2 Hz, 3H), 1.39–1.51 (m, 2H), 1.61–1.71 (m, 2H), 2.15 (s, 3H), 2.35 (s, 3H), 4.15 (t, J = 7.8 Hz, 2H), 6.98–7.03 (m, 1H), 7.25–7.30 (m, 2H), 7.41–7.45 (m, 2H), 8.03 (s, 1H). Anal. calcd for $C_{18}H_{23}N_3O_2$; C, 68.98; H, 7.40; N, 13.41. Found: C, 68.72; H, 7.35; N, 13.35.

5.1.3. *N*-Benzyl-1-butyl-5,6-dimethyl-2-oxo-1,2-dihydropyridine-3-carboxamide (13)

To a solution of **12** (223 mg, 1.0 mmol), *N*,*N*′-dicyclohexylcarbodiimide (243 mg, 1.18 mmol), and 1-hydroxybenzotriazole (20 mg, 0.15 mmol) in THF (10 mL) was added benzylamine (120 μL, 1.1 mmol), and the mixture was stirred overnight at room temperature. The reaction mixture was diluted with EtOAc and H_2O. The aqueous layer was separated and extracted with EtOAc. The combined organic extracts were washed with 1 M HCl, H_2O, and brine, dried over $MgSO_4$, filtered and concentrated. The residue was purified by flash column chromatography (silica gel, toluene/acetone = 3/1), and crystallized from CH_2Cl_2/hexane to give 12 (85 mg, 27%) as a colorless solid. Mp 73–75 °C. ^{1}H NMR (300 MHz, $CDCl_3$) δ 2.20 (s, 3H), 2.39 (s, 3H), 3.62 (s, 3H), 4.65 (d, J = 6.0 Hz, 2H), 7.21–7.38 (m, 5H), 8.37 (s, 1H), 10.28 (br s, 1H). Anal. calcd for $C_{19}H_{24}N_2O_2$: C, 73.05; H, 7.74; N, 8.97. Found: C, 72.27; H, 7.78; N, 8.95.

5.1.4. Butyl-6-ethyl-5-methyl-2-oxo-1,2-dihydropyridine-3-carboxylic acid (17a)

Compound **17a** was prepared in a similar manner as **17c**. Mp 121 °C. ^{1}H NMR (300 MHz, $CDCl_3$) δ 1.00 (t, J = 7.3 Hz, 3H), 1.27 (t, J = 7.6 Hz, 3H), 1.47 (td, J = 14.8, 7.4 Hz, 2H), 1.66–1.76 (m, 2H), 2.23 (s, 3H), 2.79 (q, J = 7.6 Hz, 2H), 4.15 (t, J = 8.1 Hz, 2H), 8.29 (s, 1H), 14.77 (s, 1H).

5.1.5. *N*-Benzyl-1-butyl-6-ethyl-5-methyl-2-oxo-1,2-dihydropyridine-3-carboxamide (18a)

Compound **18a** was prepared in a similar manner as **18c**. Mp 74–75 °C. ^{1}H NMR (300 MHz, $CDCl_3$) δ 0.98 (t, J = 7.5 Hz, 3H), 1.22 (t, J = 7.5 Hz, 3H), 1.36–1.51 (m, 2H), 1.61–1.72 (m, 2H), 2.19 (s, 3H), 2.73 (quint, J = 7.5 Hz, 2H), 4.05 (t, J = 7.8 Hz, 2H), 4.64 (d, J = 6.0 Hz, 2H), 7.20–7.39 (m, 5H), 8.35 (s, 1H), 10.03 (br s, 1H). Anal. calcd for $C_{20}H_{26}N_2O_2$: C, 73.59; H, 8.03; N, 8.58. Found: C, 73.50; H, 8.00; N, 8.57.

5.1.6. Methyl 1-butyl-2-oxo-2,5,6,7-tetrahydro-1*H*-cyclopenta[*b*]pyridine-3-carboxylate (17b)

Compound **17b** was prepared in a similar manner as **18c**. ^{1}H NMR (300 MHz, $CDCl_3$) δ 0.96 (t, J = 7.3 Hz, 3.0H), 1.40 (dt, J = 15.0, 7.4 Hz, 2.2H), 1.65–1.76 (m, 2.2H), 2.12–2.22 (m, 1.9H), 2.81 (t, J = 7.3 Hz, 2.2H), 2.98 (t, J = 7.8 Hz, 1.9H), 3.89 (s, 3.2H), 3.96 (t, J = 7.8 Hz, 2.2H), 8.09 (s, 1.0H).

5.1.7. *N*-Benzyl-1-butyl-2-oxo-2,5,6,7-tetrahydro-1*H*-cyclopenta[*b*]pyridine-3-carboxamide (18b)

Compound **18b** was prepared in a similar manner as **18c**. ^{1}H NMR (300 MHz, $CDCl_3$) δ 0.97 (t, J = 7.5 Hz, 3H), 1.41 (sextet, J = 7.5 Hz, 2H), 1.69 (quint, J = 7.5 Hz, 2H), 2.19 (quint, J = 7.5 Hz, 2H), 2.85 (t, J = 7.5 Hz, 2H), 3.00 (t, J = 7.5 Hz, 2H), 3.98 (t, J = 7.8 Hz, 2H), 4.64 (d, J = 6.0 Hz, 2H), 7.23–7.39 (m, 5H), 8.46 (s, 1H), 10.31 (br t, J = 6.0 Hz, 1H). HRMS-FAB (m/z): $[M+H]^+$ calcd for $C_{20}H_{25}N_2O_2$, 325.1911; found: 325.1914.

5.1.8. Butyl-2-oxo-1,2,5,6,7,8-hexahydroquinoline-3-carboxylic acid (17c)

A flask with a Dean–Stark apparatus was charged with cyclohexanone (10.36 mL, 0.1 mol), 1-butyl amine (9.98 mL, 0.1 mol), and toluene (15 mL). The mixture was heated to refluxing and stirred for 24 h. The solution was distilled (64 °C, 2 mmHg) to give *N*-cyclohexylidenebutan-1-amine (12.8 g, 84%) as a colorless oil. ^{1}H NMR (300 MHz, $CDCl_3$) δ 0.93 (t, J = 7.5 Hz, 3H), 1.35 (sextet, J = 7.5 Hz, 2H), 1.58 (quint, J = 7.5 Hz, 2H), 1.61–1.70 (m, 4H), 1.71–1.77 (m, 2H), 2.30 (t, J = 6.0 Hz, 2H), 2.34 (t, J = 6.0 Hz, 2H), 3.30 (t, J = 7.5 Hz, 2H). A solution of *N*-cyclohexylidenebutan-1-amine (12.8 g, 83.6 mmol) in diglyme (75 mL) was heated to 120 °C. To this solution was added a solution of dimethyl 2-(methoxymethylene)malonate (14 g, 80.4 mmol) in diglyme (75 mL) dropwise over 1 h. The mixture was stirred at 120 °C for 3 h and then evaporated. The residue was purified by column chromatography (silica gel, EtOAc/toluene 1/1) to give **16c** (15 g, 71%) a yellow oil. ^{1}H NMR (300 MHz, $CDCl_3$) δ 0.93 (t, J = 7.5, 3H). 1.43 (sextet, J = 7.5 Hz, 2H), 1.63–1.78 (m, 4H), 1.87 (quint, J = 6.0 Hz, 2H), 2.57 (t, J = 6.0 Hz, 2H), 2.73 (t, J = 6.0 Hz, 2H), 3.90 (s, 3H), 4.02 (t, J = 7.8 Hz, 2H), 7.92 (s, 1H). To a solution of **16c** (263 mg, 1 mmol) in ethanol (6 mL) was added 2 M NaOH aqueous solution (0.6 mmol, 1.2 mmol). The mixture was stirred for 30 min at room temperature, and the resulting mixture was diluted with 0.4 M HCl aqueous solution (6 mL) and EtOAc. The aqueous layer was separated and extracted with EtOAc. The combined organic extracts were washed with brine, dried over $MgSO_4$, filtered and concen-

trated. The residue was crystallized from EtOAc/hexane to give **17c** (220 mg, 88%) as a white solid. Mp 116 °C. ^{1}H NMR (300 MHz, $CDCl_3$) δ 1.00 (t, J = 7.5 Hz, 3H), 1.46 (sextet, J = 7.5 Hz, 2H), 1.68–1.73 (m, 2H), 1.77 (quint, J = 6.0 Hz, 2H), 1.92 (quint, J = 6.0 Hz, 2H), 2.65 (t, J = 6.0 Hz, 2H), 2.80 (t, J = 6.0 Hz, 2H), 4.10 (t, J = 7.8 Hz, 2H), 8.22 (s, 1H), 14.82 (s, 1H). Anal. calcd for $C_{14}H_{19}NO_3$: C, 67.45; H, 7.68; N, 5.62. Found: C, 67.19; H, 7.68; N, 5.53.

5.1.9. *N*-Benzyl-1-butyl-2-oxo-1,2,5,6,7,8-hexahydroquinoline-3-carboxamide (18c)

To a solution of **17c** (100 mg, 0.38 mmol) in toluene (3 mL) was added thionyl chloride (83 μL, 1.14 mmol), followed by DMF (one drop). The mixture was heated to 75 °C and stirred for 30 min. The mixture was allowed to cool to room temperature, and evaporated. The mixture was diluted with CH_2Cl_2, and benzyl amine (250 μL, 2.28 mmol) was added to this solution. The reaction mixture was stirred for 30 min at room temperature, and poured onto 1 M HCl aqueous solution. The mixture was extracted with EtOAc, and the combined organic extracts were washed with H_2O, dried over $MgSO_4$, filtered and concentrated. The residue was purified by flash column chromatography (silica gel, toluene/EtOAc = 6/1) to give **18c** (90 mg, 70%) as a white solid. ^{1}H NMR (300 MHz, $CDCl_3$) δ 0.97 (t, J = 7.5 Hz, 3H), 1.43 (sextet, J = 7.5 Hz, 2H), 1.62 (quint, J = 7.5 Hz, 2H), 1.74 (quint, J = 6.0 Hz, 2H), 1.88 (quint, J = 6.0 Hz, 2H), 2.62 (t, J = 6.0 Hz, 2H), 2.74 (t, J = 6.0 Hz, 2H), 4.03 (t, J = 7.8 Hz, 2H), 4.64 (d, J = 6.0 Hz, 2H), 7.23–7.38 (m, 5H), 8.28 (s, 1H), 10.32 (br t, J = 6.0 Hz, 1H). Anal. calcd for $C_{21}H_{26}N_2O_2$: C, 74.52; H, 7.74; N, 8.28. Found: C, 74.42; H, 7.73; N, 8.20.

5.1.10. Methyl 1-butyl-2-oxo-2,5,7,8-tetrahydro-1*H*-pyrano[4,3-*b*]pyridine-3-carboxylate (16d)

Compound **16d** was prepared in similar manner as **17c**. ^{1}H NMR (300 MHz, $CDCl_3$) δ 0.97 (t, J = 7.3 Hz, 3H), 1.43 (dt, J = 14.9, 7.3 Hz, 2H), 1.62–1.73 (m, 2H), 2.81 (t, J = 5.5 Hz, 2H), 3.90 (s, 3H), 3.98–4.03 (m, 4H), 4.55 (s, 2H), 7.85 (s, 1H).

5.1.11. *N*-Benzyl-1-butyl-2-oxo-2,5,7,8-tetrahydro-1*H*-pyrano[4,3-*b*]pyridine-3-carboxamide (18d)

Compound **18d** was prepared in a similar manner as **18c**. ^{1}H NMR (300 MHz, $CDCl_3$) δ 0.98 (t, J = 7.5 Hz, 3H), 1.43 (sextet, J = 7.5 Hz, 2H), 1.66 (quint, J = 7.5 Hz, 2H), 2.82 (t, J = 6.0 Hz, 2H), 4.01 (t, J = 6.0 Hz, 2H), 4.02 (t, J = 7.5 Hz, 2H), 4.60 (s, 2H), 4.64 (d, J = 6.0 Hz, 2H), 7.24–7.38 (m, 5H), 8.22 (s, 1H), 10.22 (br t, J = 6.0 Hz, 1H). HRMS-FAB (m/z): $[M+H]^+$ calcd for $C_{20}H_{25}N_2O_3$, 341.1860; found: 341.1866.

5.1.12. Butyl-2-oxo-1,2,5,6,7,8,9,10-octahydrocycloocta[*b*]pyridine-3-carboxylic acid (17e)

Compound **17e** was prepared in a similar manner as **17c**. Mp 110 °C. ^{1}H NMR (300 MHz, $CDCl_3$) δ 1.00 (t, J = 7.3 Hz, 3H), 1.40–1.50 (m, 6H), 1.66–1.73 (m, 4H), 1.76–1.84 (m, 2H), 2.67 (t, J = 6.0 Hz, 2H), 2.94 (t, J = 6.4 Hz, 2H), 4.16 (t, J = 7.8 Hz, 2H), 8.28 (s, 1H). Anal. calcd for $C_{16}H_{23}NO_3$: C, 69.29; H, 8.36; N, 5.05. Found: C, 68.97; H, 8.49; N, 5.05.

5.1.13. *N*-Benzyl-1-butyl-2-oxo-1,2,5,6,7,8,9,10-octahydrocycloocta[*b*]pyridine-3-carboxamide (18e)

Compound **18e** was prepared in a similar manner as **18c**. Mp 70 °C. ^{1}H NMR (300 MHz, $CDCl_3$) δ 0.97 (t, J = 7.5 Hz, 3H), 1.35–1.53 (m, 4H), 1.44 (sextet, J = 7.5 Hz, 2H), 1.60–1.78 (m, 6H), 2.64 (t, J = 6.0 Hz, 2H), 2.88 (t, J = 6.0 Hz, 2H), 4.09 (br t, J = 7.8 Hz, 2H), 4.64 (d, J = 6.0 Hz, 2H), 7.17–7.39 (m, 5H), 8.34 (s, 1H), 10.34 (br t, J = 6.0 Hz, 1H). Anal. calcd for $C_{23}H_{30}N_2O_2$: C, 75.37; H, 8.25; N, 7.64. Found: C, 75.39; H, 8.51; N, 7.58.

5.1.14. *N*-Benzyl-1-isopentyl-2-oxo-1,2,5,6,7,8,9,10-octahydrocycloocta[*b*]pyridine-3-carboxamide (21a)

Compound **21a** was prepared as described for **17c** and **18c**. ^{1}H NMR (300 MHz, $CDCl_3$) δ 0.99 (d, J = 6.7 Hz, 6H), 1.32–1.82 (m, 11H), 2.64 (t, J = 6.3 Hz, 2H), 2.87 (t, J = 6.3 Hz, 2H), 3.98–4.20 (br s, 2H), 4.64 (d, J = 5.8 Hz, 2H), 7.23–7.40 (m, 5H), 8.34 (s, 1H), 10.3 (br t, J = 6.0 Hz, 1H). HRMS-FAB (m/z): $[M+H]^+$ calcd for $C_{24}H_{33}N_2O_2$, 381.2537; found: 381.2540.

5.1.15. *N*-Benzyl-1-(2-methoxyethyl)-2-oxo-1,2,5,6,7,8,9,10-octahydrocycloocta[*b*]pyridine-3-carboxamide (21b)

Compound **21b** was prepared as described for **17c** and **18c**. Mp 66 °C. ^{1}H NMR (300 MHz, $CDCl_3$) δ 1.36 (quint, J = 6.0 Hz, 2H), 1.49 (quint, J = 6.0 Hz, 2H), 1.61–1.68 (m, 2H), 1.69 (quint, J = 6.0 Hz, 2H), 2.66 (t, J = 6.0 Hz, 2H), 3.03 (t, J = 5.4 Hz, 2H), 4.32 (t, J = 5.4 Hz, 2H), 4.64 (d, J = 6.0 Hz, 2H), 7.26–7.40 (m, 5H), 8.36 (s, 1H), 10.25 (br r, J = 6.0 Hz, 1H). HRMS-FAB (m/z): $[M+H]^+$ calcd for $C_{22}H_{29}N_2O_3$, 369.2178; found: 369.2178. Anal. calcd for $C_{22}H_{28}N_2O_3$: C, 71.71; H, 7.66; N, 7.60. Found: C, 71.54; H, 7.50; N, 7.54.

5.1.16. *N*-Benzyl-1-(3-morpholinopropyl)-2-oxo-1,2,5,6,7,8,9,10-octahydrocycloocta[*b*]pyridine-3-carboxamide (21c)

Compound **21c** was prepared as described for **17c** and **18c**. ^{1}H NMR (300 MHz, $CDCl_3$) δ 1.34–1.54 (m, 4H), 1.60–1.81 (m, 4H), 1.82–1.94 (m, 2H), 2.28–2.50 (m, 6H), 2.64 (t, J = 6.4 Hz, 2H), 2.93 (t, J = 6.4 Hz, 2H), 3.70 (t, J = 4.5 Hz, 2H), 4.17 (t, J = 7.5 Hz, 2H), 4.17 (t, J = 7.5 Hz, 2H), 4.64 (d, J = 5.8 Hz, 2H), 7.20–7.39 (m, 5H), 8.34 (s, 1H). 10.29 (br t, 1H). HRMS-FAB (m/z): $[M+H]^+$ calcd for $C_{26}H_{36}N_3O_3$, 438.2751; found: 438.2755.

5.1.17. Butyl-2-oxo-1,2,5,6,7,8,9,10-octahydrocycloocta[*b*]pyridine-3-carboxamide (22a)

Compound **22a** was prepared in a similar manner as **18c** after substituting **17e** for **17c**. ^{1}H NMR (300 MHz, $CDCl_3$) δ 0.99 (t, J = 7.2 Hz, 3H), 1.37–1.56 (m, 4H), 1.47 (sextet, J = 7.2 Hz, 2H), 1.63–1.81 (m, 6H), 2.64 (t, J = 6.0 Hz, 2H), 2.90 (t, J = 6.0 Hz, 2H), 4.11 (t, J = 7.2 Hz, 2H), 5.69 (br s, 1H), 8.30 (s, 1H), 9.63 (br s, 1H). HRMS-FAB (m/z): $[M+H]^+$ calcd for $C_{16}H_{25}N_2O_2$, 277.1905; found: 277.1910.

5.1.18. Butyl-*N*-isopropyl-2-oxo-1,2,5,6,7,8,9,10-octahydrocycloocta[*b*]pyridine-3-carboxamide (22b)

Compound **22b** was prepared in a similar manner as **18c** after substituting **17e** for **17c**. ^{1}H NMR (300 MHz, $CDCl_3$) δ 0.99 (t, J = 7.2 Hz, 3H), 1.26 (d, J = 6.9 Hz, 6H), 1.34–1.52 (m, 4H), 1.47 (sextet, J = 7.2 Hz, 2H), 1.60–1.80 (m, 6H), 2.65 (t, J = 6.0 Hz, 2H), 2.88 (t, J = 6.0 Hz, 2H), 4.09 (br t, J = 7.2 Hz, 2H), 4.25 (sextet, J = 6.6 Hz, 1H), 8.31 (s, 1H), 9.82 (br s, 1H). HRMS-FAB (m/z): $[M+H]^+$ calcd for $C_{19}H_{31}N_2O_2$, 319.238; found: 319.2384.

5.1.19. Butyl-*N*-cyclohexyl-2-oxo-1,2,5,6,7,8,9,10-octahydrocycloocta[*b*]pyridine-3-carboxamide (22c)

Compound **22c** was prepared in a similar manner as **18c** after substituting **17e** for **17c**. Mp 90 °C. ^{1}H NMR (300 MHz, $CDCl_3$) δ 0.99 (t, J = 7.2 Hz, 3H), 1.20–1.53 (m, 12H), 1.59–1.80 (m, 8H), 1.95–2.01 8 m, 2H), 2.63 (t, J = 6.0 Hz, 2H), 2.88 (t, J = 6.0 Hz, 2H), 3.91–4.02 (m, 1H), 4.09 (br t, J = 7.2 Hz, 2H), 8.30 (s, 1H), 9.88 (d, J = 7.5 Hz, 1H). HRMS-FAB (m/z): $[M+H]^+$ calcd for $C_{22}H_{35}N_2O_2$, 359.2693; found: 359.2690.

5.1.20. Butyl-*N*-(1-methylpiperidin-4-yl)-2-oxo-1,2,5,6,7,8,9,10-octahydrocycloocta[*b*]pyridine-3-carboxamide (22d)

Compound **22d** was prepared in a similar manner as **18c** after substituting **17e** for **17c**. ^{1}H NMR (300 MHz, $CDCl_3$) δ 0.99 (t, J = 7.2 Hz, 3H), 1.38–1.50 (m, 4H), 1.47 (quint, J = 7.2 Hz, 2H), 1.64–1.82 (m, 8H), 2.01–2.09 (m, 2H), 2.25–2.34 (m, 2H), 2.35 (s, 3H), 2.64 (t, J = 6.0 Hz, 2H), 2.82–2.90 (m, 2H), 2.88 (t, J = 6.0 Hz, 2H), 3.97–4.06 (m, 1H), 4.10 (br t, J = 7.2 Hz, 2H), 8.28 (s, 1H), 9.98 (d, J = 7.2 Hz, 1H). HRMS-FAB (m/z): $[M+H]^+$ calcd for $C_{22}H_{36}N_3O_2$, 374.2802; found: 374.2797.

5.1.21. Butyl-2-oxo-*N*-(2-phenylpropan-2-yl)-1,2,5,6,7,8,9,10-octahydrocycloocta[*b*]pyridine-3-carboxamide (22e)

Compound **22e** was prepared in a similar manner as **18c** after substituting **17e** for **17c**. ^{1}H NMR (300 MHz, $CDCl_3$) δ 1.00 (t, J = 7.2 Hz, 3H), 1.30–1.55 (m, 6H), 1.59 (s, 6H), 1.56–1.89 (m, 6H), 1.59 (s, 6H), 1.56–1.89 (m, 6H), 2.58 (t, J = 6.0 Hz, 2H), 2.88 (t, J = 6.3 Hz, 2H), 4.00–4.23 (m, 2H), 7.10–7.40 (m, 5H), 7.46 (d, J = 8.4 Hz, 2H), 8.23 (s, 1H). HRMS-FAB (m/z): $[M+H]^+$ calcd for $C_{25}H_{35}N_2O_2$, 395.2693; found: 395.2697.

5.1.22. Butyl-2-oxo-*N*-phenethyl-1,2,5,6,7,8,9,10-octahydrocycloocta[*b*]pyridine-3-carboxamide (22f)

Compound **22f** was prepared in a similar manner as **18c** after substituting **17e** for **17c**. ^{1}H NMR (300 MHz, $CDCl_3$) δ 0.99 (t, J = 7.5 Hz, 3H), 1.34–1.53 (m, 4H), 1.46 (sextet, J = 7.5 Hz, 2H), 1.62–1.80 (m, 6H), 2.64 (t, J = 6.0 Hz, 2H), 2.89 (t, J = 6.0 Hz, 2H), 2.94 (t, J = 7.5 Hz, 2H), 3.67 (dt, J = 9.0, 6.0 Hz, 2H), 4.10 (br t, J = 7.8 Hz, 2H), 7.18–7.34 (m, 5H), 8.31 (s, 1H), 10.07 (br t, J = 6.0 Hz, 1H). HRMS-FAB (m/z): $[M+H]^+$ calcd for $C_{24}H_{33}N_2O_2$, 381.2537; found: 381.2530.

5.2. Biology

5.2.1. CB2/CB1 binding and cell-based cAMP assays

The CB1/CB2 binding assay and cell-based cAMP assay were performed as described in Ref. 17a. In brief, the binding activities of compounds were evaluated from their competition binding against [^{3}H]-CP-55,940.[11,12] The cell membranes were prepared from Chinese hamster ovary (CHO) cells stably expressed recombinant human CB1 or CB2, or mouse brain (mouse CB1) or spleen (mouse CB2). The functional activities of the selected compounds were assessed by the inhibition effect on the forskolin-evoked cAMP accumulation in CHO cells expressing human CB2.[13] IC_{50} was determined by more than four duplicate assay points. The between-day coefficients of variation values of human CB1, CB2 binding, and cAMP assay were 0.24 (compound **11** in Ref. 17a), 0.53 (WIN-55,212-2), and 0.63 (WIN-55,212-2), respectively.

5.2.2. Anti-pruritic assay

This assay was carried out using the method of Inagaki et al.[16] Briefly, the backs of female ICR strain mice were clipped, and compound 48/80 (3 μg/50 μL/site) was injected intradermally to elicit the response. The number of scratching behaviors to the injection site by hind paws, which was observed from immediately after the injection, was counted for 30 min. A series of these behaviors was counted as one incidence of scratching, since mice generally showed several scratches in one bout. Test compounds dissolved in sesame oil or suspended in 0.5% methylcellulose were orally administered once (n = 6), and then pruritus was elicited by the injection of compound 48/80 at a pre-determined time when the maximal plasma concentration of the compound was obtained. Evaluation of the inhibitory effect against pruritus was performed by comparing the number of scratchings in the compound-administered group with that in the vehicle-administered group. The statistical analysis was carried out using Dunnett's t-test, and a p-value less than 0.05 was considered to be statistically significant.

Acknowledgments

We thank Naoki Yoshikawa for early input into this work and useful discussions, Yuka Iwamoto and Akihiro Matsuda for the pharmacokinetic studies, Rikio Ikenishi and Yumiko Takagi for the elemental analysis, and Shinya Yoshimatsu for the HRMS analysis. K.K. also acknowledges Robert Hall for his assistance in preparing this manuscript.

References and notes

1. Patel, T.; Yosipovitch, G. *Expert Opin. Pharmacother.* **2010**, *11*, 1673.
2. Ikoma, A.; Steinhoff, M.; Staender, S.; Yosipovitch, G.; Schmelz, M. *Nat. Rev. Neurosci.* **2006**, *7*, 535.
3. Yosipovitch, G.; Papoiu, A. D. P. *Curr. Allergy Asthma Rep.* **2008**, *8*, 306.
4. Stakeholder Opinions: Atopic dermatitis; DMHC2279; Datamonitor: New York, March 2007.
5. Dvorak, M.; Watkinson, A.; McGlone, F.; Rukwied, R. *Inflamm. Res.* **2003**, *52*, 238.
6. Maekawa, T.; Nojima, H.; Kuraishi, Y.; Aisaka, K. *Eur. J. Pharmacol.* **2006**, *542*, 179.
7. Hanus, L.; Breuer, A.; Tchilibon, S.; Shiloah, S.; Goldenberg, D.; Horowitz, M.; Pertwee, R. G.; Ross, R. A.; Mechoulam, R.; Fride, E. *Proc. Natl. Acad. Sci. U.S.A.* **1999**, *96*, 14228.
8. Malan, T. P., Jr.; Ibrahim, M. M.; Deng, H.; Liu, Q.; Mata, H. P.; Vanderah, T.; Porreca, F.; Makriyannis, A. *Pain* **2001**, *93*, 239.
9. (a) Huffman, J. W.; Lu, J.; Hynd, G.; Wiley, J. L.; Martin, B. R. *Bioorg. Med. Chem.* **2001**, *9*, 2863; (b) Giblin, G. M. P.; O'Shaughnessy, C. T.; Naylor, A.; Mitchell, W. L.; Eatherton, A. J.; Slingsby, B. P.; Rawlings, D. A.; Goldsmith, P.; Brown, A. J.; Haslam, C. P.; Clayton, N. M.; Wilson, A. W.; Chessell, I. P.; Wittington, A. R.; Green, R. *J. Med. Chem.* **2007**, *50*, 2597; (c) Giblin, G. M. P.; Billinton, A.; Briggs, M.; Brown, A. J.; Chessell, I. P.; Clayton, Nick M.; Eatherton, Andrew J.; Goldsmith, P.; Haslam, C.; Johnson, M. R.; Mitchell, W. L.; Naylor, A.; Perboni, A.; Slingsby, B. P.; Wilson, A. W. *J. Med. Chem.* **2009**, *52*, 5785; (d) Cheng, Y.; Albrecht, B. K.; Brown, J.; Buchanan, J. L.; Buckner, W. H.; DiMauro, E. F.; Emkey, R.; Fremeau, R. T.; Harmange, J.-C.; Hoffman, B. J.; Huang, L.; Huang, M.; Lee, J. H.; Lin, F.-F.; Martin, M. W.; Nguyen, H. Q.; Patel, V. F.; Tomlinson, S. A.; White, R. D.; Xia, X.; Hitchcock, S. A. *J. Med. Chem.* **2008**, *51*, 5019; (e) van der Stelt, M.; Cals, J.; Broeders-Josten, S.; Cottney, J.; van der Doelen, A. A.; Hermkens, M. L.; de Kimpe, V.; King, A.; Klomp, J.; Oosterom, J.; Pols-de Rooij, I.; de Roos, J.; van Tilborg, M.; Boyce, S.; Baker, J. *J. Med. Chem.* **2011**, *54*, 7350; (f) Frost, J. M.; Dart, M. J.; Tietje, K. R.; Garrison, T. R.; Grayson, G. K.; Daza, A. V.; El-Kouhen, O. F.; Yao, B. B.; Hsieh, G. C.; Pai, M.; Zhu, C. Z.; Chandran, P.; Meyer, M. D. *J. Med. Chem.* **2010**, *53*, 295; (g) Frost, J. M.; Dart, M. J.; Tietje, K. R.; Garrison, T. R.; Grayson, G. K.; Daza, A. V.; El-Kouhen, O. F.; Miller, L. N.; Li, L.; Yao, B. B.; Hsieh, G. C.; Pai, M.; Zhu, C. Z.; Chandran, P.; Meyer, M. D. *J. Med. Chem.* **2008**, *51*, 1904; (h) Stern, E.; Muccioli, G. G.; Millet, R.; Goossens, J.-F.; Farce, A.; Chavatte, P.; Poupaert, J. H.; Lambert, D. M.; Depreux, P.; Henichart, J.-P. *J. Med. Chem.* **2006**, *49*, 70; (i) Stern, E.; Muccioli, G. G.; Bosier, B.; Hamtiaux, L.; Millet, R.; Poupaert, J. H.; Henichart, J.-P.; Depreux, P.; Goossens, J.-F.; Lambert, D. M. *J. Med. Chem.* **2007**, *50*, 5471.
10. Kusakabe, K.-i.; Tada, Y.; Iso, Y.; Sakagami, M.; Morioka, Y.; Chomei, N.; Shinonome, S.; Kawamoto, K.; Takenaka, H.; Yasui, K.; Hamana, H.; Hanasaki, K. *Bioorg. Med. Chem.* **2013**, *21*, 2045.
11. Compton, D. R.; Rice, K. C.; De Costa, B. R.; Razdan, R. K.; Melvin, L. S. *J. Pharmacol. Exp. Ther.* **1993**, *265*, 218.
12. Showalter, V. M.; Compton, D. R.; Martin, B. R.; Abood, M. E. *J. Pharmacol. Exp. Ther.* **1996**, *278*, 989.
13. Pertwee, R. *Gen. Pharmacol. Vasc. Syst.* **1993**, *24*, 811.
14. Rasmussen, S. G. F.; DeVree, Brian T.; Zou, Y.-Z.; Kruse, A. C.; Chung, K.-Y.; Kobilka, T.-S.; Thian, F.-S.; Chae, P.-S.; Pardon, E.; Calinski, D.; Mathiesen, J. M.; Shah, S. T. A.; Lyons, J. A.; Caffrey, M.; Gellman, S. H.; Steyaert, J.; Skiniotis, G.; Weis, W. I.; Sunahara, R. K.; Kobilka, B. K. *Nature* **2011**, *477*, 549.
15. (a) Goto, J.; Kataoka, R.; Muta, H.; Hirayama, N. *J. Chem. Inf. Model.* **2008**, *48*, 583; (b) ASEDock Version RSI2010.07.14; Ryoka Systems: Tokyo, Japan.
16. Inagaki, N.; Nakamura, N.; Nagao, M.; Musoh, K.; Kawasaki, H.; Nagai, H. *Eur. J. Pharmacol.* **1999**, *367*, 361.
17. (a) Kai, H.; Morioka, Y.; Murashi, T.; Morita, K.; Shinonome, S.; Nakazato, H.; Kawamoto, K.; Hanasaki, K.; Takahashi, F.; Mihara, S.; Arai, T.; Abe, K.; Okabe, H.; Baba, T.; Yoshikawa, T.; Takenaka, H. *Bioorg. Med. Chem. Lett.* **2007**, *17*, 4030; (b) Kai, H.; Morioka, Y.; Tomida, M.; Takahashi, T.; Hattori, M.; Hanasaki, K.; Koike, K.; Chiba, H.; Shinohara, S.; Kanemasa, T.; Iwamoto, Y.; Takahashi, K.; Yamaguchi, Y.; Baba, T.; Yoshikawa, T.; Takenaka, H. *Bioorg. Med. Chem. Lett.* **2007**, *17*, 3925; (c) Kai, H.; Morioka, Y.; Koriyama, Y.; Okamoto, K.; Hasegawa, Y.; Hattori, M.; Koike, K.; Chiba, H.; Shinohara, S.; Iwamoto, Y.; Takahashi, K.; Tanimoto, N. *Bioorg. Med. Chem. Lett.* **2008**, *18*, 6444.
18. Odan, M.; Ishizuka, N.; Hiramatsu, Y.; Inagaki, M.; Hashizume, H.; Fujii, Y.; Mitsumori, S.; Morioka, Y.; Soga, M.; Deguchi, M.; Yasui, K.; Arimura, A. *Bioorg. Med. Chem. Lett.* **2012**, *22*, 2803.

19. Odan, M.; Ishizuka, N.; Hiramatsu, Y.; Inagaki, M.; Hashizume, H.; Fujii, Y.; Mitsumori, S.; Morioka, Y.; Soga, M.; Deguchi, M.; Yasui, K.; Arimura, A. *Bioorg. Med. Chem. Lett.* **2012**, *22*, 2898.
20. Ballesteros, J. A.; Weinstein, H. W. In *Methods in Neuroscience*; Conn, P. M., Sealfon, S. C., Eds.; Academic Press: San Diego, 1995; Vol. 25, p 366.
21. PyMOL, Version 0.98; DeLano Scientific: San Carlos, CA, USA.